# High Output Saturation and High-Linearity Uni-Traveling-Carrier Waveguide Photodiodes

Jonathan Klamkin, *Student Member, IEEE*, Anand Ramaswamy, *Student Member, IEEE*, Leif A. Johansson, *Member, IEEE*, Hsu-Feng Chou, *Member, IEEE*, Matthew N. Sysak, *Member, IEEE*, James W. Raring, *Student Member, IEEE*, Navin Parthasarathy, Steven P. DenBaars, *Fellow, IEEE*, John E. Bowers, *Fellow, IEEE*, and Larry A. Coldren, *Fellow, IEEE*

***Abstract*—Waveguide uni-traveling-carrier photodiodes (UTC-PDs) have been fabricated and tested. Output saturation currents greater than 40 mA at 1 GHz are demonstrated for a 10 $\mu$m $\times$ 150 $\mu$m photodiode (PD). The third-order intermodulation distortion is also measured and exhibits a third-order output intercept point of 43 dBm at 20 mA and 34 dBm at 40 mA for this same PD. UTC-PDs with geometries of 5 $\mu$m $\times$ 100 $\mu$m and 10 $\mu$m $\times$ 100 $\mu$m are also compared and it is shown that a wider waveguide PD has improved saturation characteristics due to the lower optical power density which reduces the saturation at the front end of the device.**

***Index Terms*—Fiber-optic link, linearity, photodiode (PD), saturation current, third-order intermodulation distortion (IMD3), third-order output intercept point (OIP3), uni-traveling-carrier photodiode (UTC-PD).**

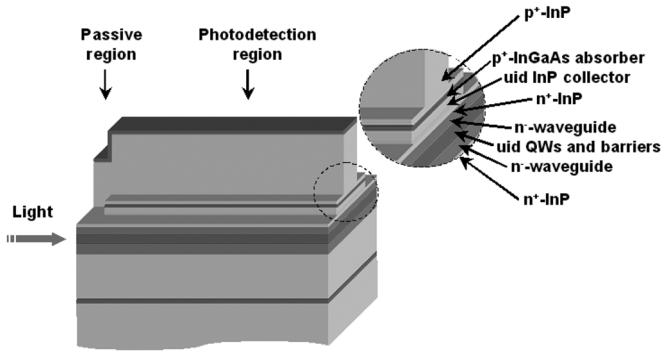


Fig. 1. Device schematic of UTC-PD.

## I. Introduction

HIGH-POWER photodetectors are required for high-performance analog fiber-optic links. To increase the spur-free dynamic range (SFDR), high transmitted optical power can be used in conjunction with high saturation power and high-linearity photodetectors [1]. Coherent fiber-optic links have the potential to further improve SFDR, however, the limiting factor to achieving high linearity is the optical receiver. In [2], a coherent receiver with feedback to a local tracking phase modulator has been proposed to significantly enhance the linearity of the phase demodulator and in turn the SFDR of the link. For successful operation at high frequency, the delay of this feedback must be kept short. With a monolithically integrated receiver, operation at 1 GHz is feasible. For such a coherent receiver, a balanced photodiode (PD) configuration can be utilized for shot noise limited operation, and this balanced PD should be integrated with a coupler for mixing the received radio-frequency (RF) signal with a local oscillator wave, and a local tracking phase modulator. Therefore, it is desirable to fabricate high-power and high-linearity photodetectors that can operate at 1 GHz and can be monolithically integrated with other optical components such as couplers and phase modulators. It is imperative that a waveguide PD is employed. Waveguide p-i-n photodetectors have been reported with an OIP3 of 27 dBm at 20 mA of photocurrent and a frequency of 20 GHz [3]. Uni-traveling-carrier photodiodes (UTC-PDs) have the potential for improved saturation current and linearity because of reduced space charge effects [4]. UTC-PDs have demonstrated an OIP3 of 37.5 dBm at 22 mA and around 5.8 GHz [5] and 30 dBm at 21.3 mA and 40 GHz [6]. Because the *RC* requirements are relaxed for operation at 1 GHz, the PD can be designed for higher saturation current and higher linearity.

An advanced device architecture has recently been developed allowing for the monolithic integration of UTC-PDs with low loss passive waveguides and quantum-well (QW)-based components [7]. In this letter, we report waveguide UTC-PDs that demonstrate both high saturation current and high linearity at a frequency of 1 GHz. To the best of our knowledge, the OIP3 values obtained for these PDs are the highest reported for a waveguide PD at comparable frequencies. These UTC-PDs are fabricated on a platform that readily allows for the integration of other optical components such as optical phase modulators and multimode interference couplers. The saturation current was characterized by measuring the optical-to-electrical frequency response of the PDs at varying photocurrent levels, and the third-order intermodulation distortion (IMD3) was measured using a two-tone setup [8].

## II. Device Design

A schematic of the UTC-PD structure is shown in Fig. 1. The structure is grown on a semi-insulating InP substrate by MOCVD. The optical waveguide consists of unintentionally doped (uid) InGaAsP QWs and barriers sandwiched between

Manuscript received September 1, 2006; revised November 13, 2006. This work was supported by Defense Advanced Research Projects Agency (DARPA) through the PHORFRONT Program under U.S. Air Force Contract FA8750-05-C-0265.

The authors are with the Materials Department and the Electrical and Computer Engineering Department at the University of California, Santa Barbara, CA 93116 USA (e-mail: klamkin@engineering.ucsb.edu).

Digital Object Identifier 10.1109/LPT.2006.890101

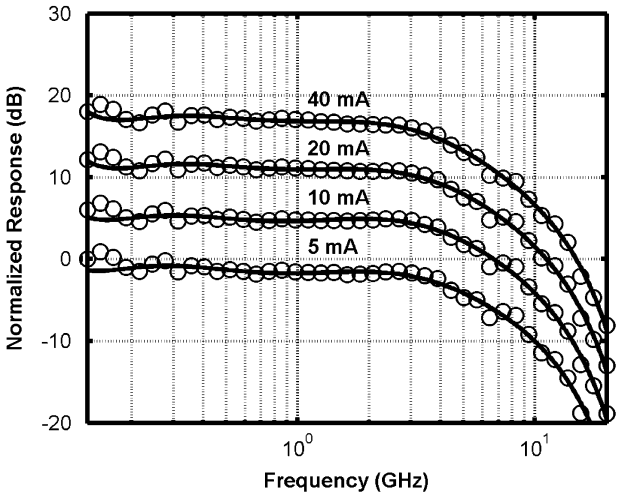


Fig. 2. Normalized response of a 10 $\mu$m × 150 $\mu$m UTC-PD at various photocurrent levels. The bias voltage is −5 V.

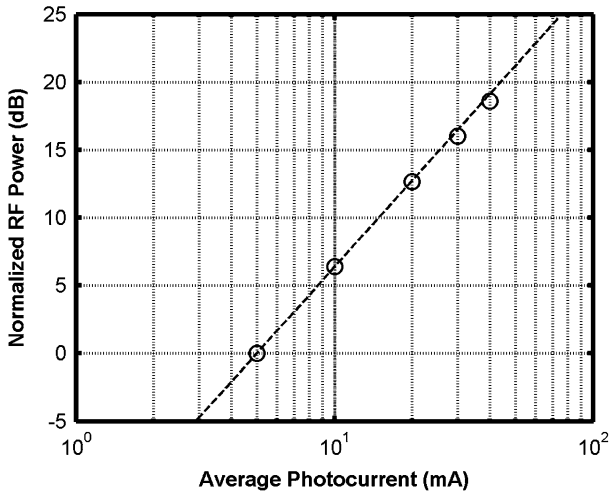


Fig. 3. Normalized RF power as a function of average photocurrent at 1 GHz for a 10 $\mu$m × 150 $\mu$m UTC-PD. The bias voltage is −5 V.

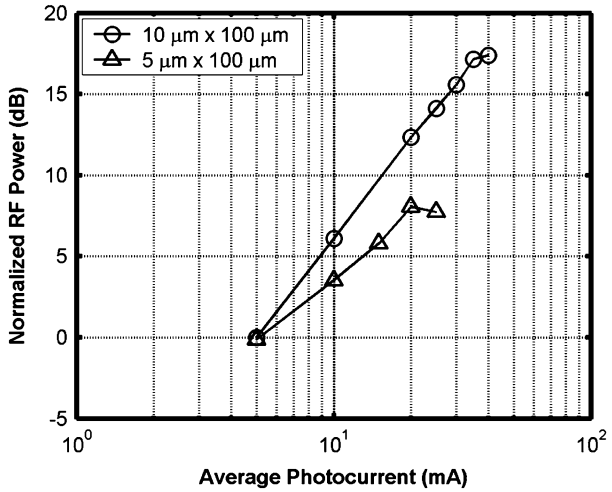


Fig. 4. Normalized RF power as a function of average photocurrent at 1 GHz for a 10 $\mu$m × 100 $\mu$m and a 5 $\mu$m × 100 $\mu$m UTC-PD. The bias voltage is −6 V for both devices.

two lightly n-doped InGaAsP waveguide layers. The UTC-PD structure grown above the optical waveguide consists of a highly n-doped InP layer, a uid InP collector, some band smoothing layers, and a highly p-doped InGaAs absorber. Photodetection regions are formed by selectively removing these UTC-PD layers. The highly n-doped InP layer serves to terminate the field on the n-side of the InP collector in the photodetection regions and prevents the applied field from depleting the optical waveguide below. After forming these regions, a p-cladding regrowth is performed. Fabricated PDs consist of a short passive region, where the UTC layers have been removed, followed by a photodetection region. Light is coupled from an optical fiber to the waveguide in the short passive region. Because the device area can be made larger, the overlap of the optical mode in the absorber is lower than that in [7] resulting in a longer absorption profile and in turn a more uniform distribution of carriers. The PDs are made longer to compensate for any potential loss in quantum efficiency. Although the regions with UTC layers removed serve as passive regions in these experiments, they can also be used as modulation regions. With this single regrowth process, several components can be monolithically integrated to form more highly functional photonic circuits such as the coherent receiver described in the introduction.

Following regrowth, ridges are formed. Topside n- and p-contacts are then deposited and annealed. Benzocyclobutene dielectric is used for reducing parasitic pad capacitance. UTC-PDs were fabricated with width by length geometries of 5 $\mu$m × 100 $\mu$m, 10 $\mu$m × 100 $\mu$m, and 10 $\mu$m × 150 $\mu$m.

## III. Experiment and Results

Optical-to-electrical frequency response measurements were performed with a lightwave component analyzer. The optical output of the lightwave component analyzer was amplified with an erbium-doped fiber amplifier (EDFA) and then coupled to the PDs using single-mode lensed fiber. The frequency response was measured at various bias voltages and photocurrent levels. The normalized response for a 10 $\mu$m × 150 $\mu$m PD is shown in Fig. 2 for up to 40 mA of photocurrent. The bias voltage for these measurements was set to −5 V. The response does not appear to degrade for the measured levels of photocurrent. Fig. 3 shows the normalized RF power as a function of average photocurrent along with a line fit through the first few points. For this device, the saturation current is greater than 40 mA. Fig. 4 shows a plot of the normalized RF power as a function of average generated photocurrent at 1 GHz for both a 10 $\mu$m × 100 $\mu$m and a 5 $\mu$m × 100 $\mu$m UTC-PD. In both cases, the bias voltage was set to −6 V. These devices are compared because they have equal length and subsequently the same quantum efficiency of around 94%. From this measurement, it is clear that the output saturation current level is significantly higher for the wider device.

To measure the IMD3 of the UTC-PDs, a two-tone setup was used similar to that in [8]. Two distributed feedback lasers were externally modulated; one at a frequency of 0.8 GHz and the other at 1.0 GHz. The signals were combined, and an EDFA was used to vary the optical power input to the PD. The IMD3 measurements for the 10 $\mu$m × 150 $\mu$m PD are shown in Fig. 5. The input electrical modulation power was varied and the data points

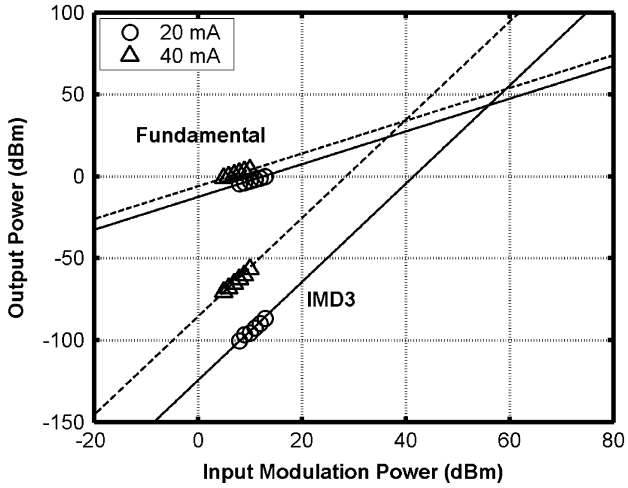


Fig. 5. IMD3 measurements for a 10 $\mu$m $\times$ 150 $\mu$m UTC-PD. At 20 mA, the bias voltage is $-8$ V and at 40 mA the bias voltage is $-5.8$ V.

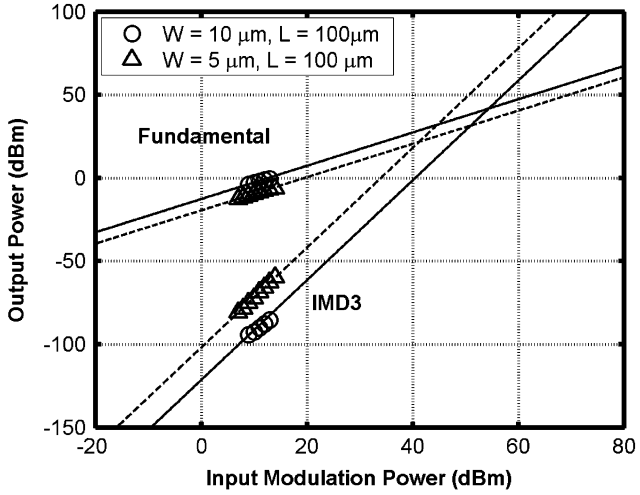


Fig. 6. IMD3 measurements for a 10 $\mu$m $\times$ 100 $\mu$m and a 5 $\mu$m $\times$ 100 $\mu$m UTC-PD. The bias voltage is $-6$ V and the photocurrent level is 20 mA.

shown correspond to a range of around 40%–75% modulation index. These measurements are for a bias of $-8$ V and a photocurrent level of 20 mA, and a bias of $-5.8$ V and a photocurrent level of 40 mA. The OIP3 for these settings was measured to be 43 and 34 dBm, respectively. To the best of our knowledge, these are the highest OIP3 values reported for a waveguide PD. Fig. 6 shows the IMD3 measurements for the 10 $\mu$m $\times$ 100 $\mu$m and the 5 $\mu$m $\times$ 100 $\mu$m PDs. For these measurements, the bias voltage was $-6$ V and the photocurrent level was 20 mA. The OIP3 for the 10 $\mu$m $\times$ 100 $\mu$m PD is 42 dBm and that for the 5 $\mu$m $\times$ 100 $\mu$m PD is 22 dBm. The OIP3 for the wider PD is much higher than that for the narrower PD, which is consistent with the saturation currents observed for these devices. This enhancement is due in part to the reduced power density in the wider PDs, which spreads the generation at the front end of the device. According to simulation, nearly 50% of the light is absorbed in the first 25 $\mu$m of length, therefore it is advantageous to reduce the power density at the front end in order to reduce space charge saturation in this region of the device.

## IV. Conclusion

We have fabricated and tested waveguide UTC-PDs that demonstrate high-saturation currents and high linearity. A 10 $\mu$m $\times$ 150 $\mu$m UTC-PD has a saturation current greater than 40 mA and OIP3 values of 43 and 34 dBm at photocurrent levels of 20 and 40 mA, respectively. Comparing devices of different widths, a 10 $\mu$m $\times$ 100 $\mu$m UTC-PD has a saturation current near 40 mA and an OIP3 of 42 dBm at 20 mA and $-6$ V, whereas a 5 $\mu$m $\times$ 100 $\mu$m UTC-PD has a much lower saturation current and an OIP3 of 22 dBm at the same operating conditions. This difference is believed to be due in part to the reduced power density at the front end of the device for the wider PD.

## References

[1] K. J. Williams, L. T. Nichols, and R. D. Esman, "Photodetector nonlinearity limitations on a high-dynamic range 3 GHz fiber optic link," *J. Lightw. Technol.*, vol. 16, no. 2, pp. 192–199, Feb. 1998.

[2] H.-F. Chou, A. Ramaswamy, D. Zibar, L. A. Johansson, J. E. Bowers, M. Rodwell, and L. Coldren, "SFDR improvement of a coherent receiver using feedback," in *Coherent Optical Technologies and Applications Conf. (COTA)*, Whistler, Canada, 2006.

[3] D. C. Scott, T. A. Vang, J. Elliott, D. Forbes, J. Lacey, K. Everett, F. Alvarex, R. Johnson, A. Krispin, J. Brock, L. Lembo, H. Jiang, D. S. Shin, J. T. Zhu, and P. K. L. Yu, "Measurement of IP3 in p-i-n photodetectors and proposed performance requirements for RF fiber-optic links," *IEEE Photon. Technol. Lett.*, vol. 12, no. 4, pp. 422–424, Apr. 2000.

[4] T. Ishibashi, T. Furuta, H. Fushimi, S. Kodama, H. Ito, T. Nagatsuma, N. Shimizu, and Y. Miyamoto, "InP/InGaAs uni-traveling-carrier photodiodes," *IEICE Trans. Electron.*, vol. E83-C, pp. 938–949, Jun. 2000.

[5] T. Ohno, H. Fukano, Y. Muramoto, T. Ishibashi, T. Yoshimatsu, and Y. Doi, "Measurement of intermodulation distortion in a unitraveling-carrier refracting-facet photodiode and a p-i-n refracting-facet photodiode," *IEEE Photon. Technol. Lett.*, vol. 14, no. 3, pp. 375–377, Mar. 2002.

[6] T. Ohno, H. Fukano, and Y. Muramoto, "Measurement of intermodulation distortion in high-output-power uni-traveling-carrier refracting-facet photodiode at 40 GHz," *Electron. Lett.*, vol. 36, pp. 1954–1955, Nov. 2000.

[7] J. W. Raring, E. J. Skogen, C. S. Wang, J. S. Barton, G. B. Morrison, S. Demiguel, S. P. DenBaars, and L. A. Coldren, "Design and demonstration of novel QW intermixing scheme for the integration of UTC-type photodiodes with QW-based components," *IEEE J. Quantum Electron.*, vol. 42, no. 2, pp. 171–181, Feb. 2006.

[8] H. Jiang, D. S. Shin, G. L. Li, T. A. Vang, D. C. Scott, and P. K. L. Yu, "The frequency behavior of the third-order-intercept point in a waveguide photodiode," *IEEE Photon. Technol. Lett.*, vol. 12, no. 5, pp. 540–542, May 2000.